Selenium prevents diabetes-induced alterations in $[Zn^{2+}]_i$ and metallothionein level of rat heart via restoration of cell redox cycle

Murat Ayaz and Belma Turan

Department of Biophysics, School of Medicine, Ankara University, Ankara, Turkey

Submitted 15 July 2005; accepted in final form 8 September 2005

Ayaz, Murat, and Belma Turan. Selenium prevents diabetes-induced alterations in $[Zn^{2+}]_i$ and metallothionein level of rat heart via restoration of cell redox cycle. *Am J Physiol Heart Circ Physiol* 290: H1071–H1080, 2006. First published October 7, 2005; doi:10.1152/ajpheart.00754.2005.—Intracellular free zinc concentration ($[Zn^{2+}]_i$) is very important for cell functions, and its excessive accumulation is cytotoxic. $[Zn^{2+}]_i$ can increase rapidly in cardiomyocytes because of mobilization of Zn^{2+} from intracellular stores by reactive oxygen species (ROS). Moreover, ROS have been proposed to contribute to direct and/or indirect damage to cardiomyocytes in diabetes. To address these hypotheses, we investigated how elevated $[Zn^{2+}]_i$ in cardiomyocytes could contribute to diabetes-induced alterations in intracellular free calcium concentration ($[Ca^{2+}]_i$). We also investigated its relationship to the changes of metallothionein (MT) level of the heart. Cardiomyocytes from normal rats loaded with fura-2 were used to fluorometrically measure resting $[Zn^{2+}]_i$ (0.52 ± 0.06 nM) and $[Ca^{2+}]_i$ (26.53 ± 3.67 nM). Fluorescence quenching by the heavy metal chelator *N,N,N',N'*-tetrakis(2-pyridylmethyl)ethylenediamine was used to quantify $[Zn^{2+}]_i$. Our data showed that diabetic cardiomyocytes exhibited significantly increased $[Zn^{2+}]_i$ (0.87 ± 0.05 nM) and $[Ca^{2+}]_i$ (49.66 ± 9.03 nM), decreased levels of MT and reduced glutathione, increased levels of lipid peroxidation and nitric oxide products, and decreased activities of superoxide dismutase, glutathione reductase, and glutathione peroxidase. Treatment (4 wk) of diabetic rats with sodium selenite (5 μmol·kg body wt^{-1}·day^{-1}) prevented these defects induced by diabetes. A comparison of present data with previously observed beneficial effects of selenium treatment on diabetes-induced contractile dysfunction of the heart can suggest that an increase in $[Zn^{2+}]_i$ may contribute to oxidant-induced alterations of excitation-contraction coupling in diabetes. In addition, we showed that oxidative stress is involved in the etiology of diabetes-induced downregulation of heart function via depressed endogenous antioxidant defense mechanisms.

intracellular zinc; intracellular calcium; Type 1 diabetes; antioxidant; oxidant stress

CARDIAC DYSFUNCTION, independent of arteriosclerosis, is one of complications in diabetes mellitus, and diabetic cardiomyopathy causes a wide range of structural and functional abnormalities (21, 27). Alteration of Ca^{2+} signaling via changes in critical processes that regulate intracellular free Ca^{2+} concentration ($[Ca^{2+}]_i$) has become a hallmark of cardiomyopathy. Although the regulation of the $[Ca^{2+}]_i$ in the myocardium is a critical determinant of contractile performance, current controversies and conclusions are available regarding the specific alterations in Ca^{2+} signaling pathways that contribute to these cardiac defects during diabetes mellitus (30, 48). Thus the molecular mechanisms of cardiac dysfunction in diabetes are not fully clarified.

Reactive oxygen species (ROS) are continuously produced in most cells under physiological conditions, and a number of enzymes and physiological antioxidants regulate their levels. Evidence implicates hyperglycemia-derived oxygen free radicals and dysregulation of nitric oxide (NO) as mediators of diabetic complications (6, 9, 43). However, as the production of ROS becomes excessive, oxidative and nitrosative stress will develop, causing functional alterations of biological tissue, and are implicated in the pathogenesis of heart failure in diabetes (12, 23, 32, 50). A number of ways have been suggested in which the damaging effect of hyperglycemia can be mediated or enhanced by ROS. For instance, hyperglycemia stimulates the production of advanced glycosylated products and enhances the polyol pathway, leading to increased superoxide anion formation (49, 55), and degrades antioxidant enzyme defenses, thereby allowing ROS to damage other enzymes and structural proteins (11, 12).

Although there are no direct data related with the alteration of concentration and distribution of intracellular free Zn^{2+} concentration ($[Zn^{2+}]_i$) and increased oxidative stress, nitrosative stress, and dysregulation of NO in isolated cardiomyocytes from diabetic rats, Bossy-Wetzel et al. (8) have also discussed the cross talk between NO and Zn^{2+} pathway to cell death involving p38-activated K^+ channels due to formation of peroxynitrite and consequent Zn^{2+} release from intracellular stores. Zinc, having multiple functions, is an essential element for living organisms. It is likely that any mechanism that alters the concentration and distribution of $[Zn^{2+}]_i$ in cardiomyocytes will cause profound functional effects. Evidence for this was provided by extracellular Zn^{2+} influx and attendant increases in $[Zn^{2+}]_i$ of some cell types (1). We and other researchers (36, 40, 42, 56) previously showed that $[Zn^{2+}]_i$ could also increase rapidly in cardiomyocytes and endothelial cells as a result of the mobilization of Zn^{2+} from intracellular stores by ROS (36, 40, 42, 56). All these observations can demonstrate a close relationship between both increased and deleterious effects of $[Zn^{2+}]_i$ and oxidant stress under diseased states of the heart. Desilet's laboratory (57) also has demonstrated the importance of increased $[Zn^{2+}]_i$ in cardiomyocytes due to its contribution to oxidant-induced alterations of excitation-contraction coupling and, if overlooked, its significant role in overestimation of $[Ca^{2+}]_i$ (57). Therefore, a study on $[Zn^{2+}]_i$ in cardiomyocytes isolated from diabetic rats will provide important and further information related to current controversies and conclusions regarding the specific alterations in Ca^{2+} signaling pathways to contribute to these cardiac defects during diabetes.

In relatively recent studies (13, 45, 61), authors demonstrated that Zn^{2+} inhibited ryanodine binding to sarcoplasmic

---

reticulum vesicles in cardiac muscle and has an inhibitory effect in intracellular Ca^{2+} release mechanisms in both smooth and skeletal muscle preparations as well as cardiomyocytes. One recent and important study (19) pointed out the loss of membrane potential and elevation of ROS in rat brain by an increased level of Zn^{2+}. In a minireview article, Viarengo and Nicotera (60) discussed the cytotoxic effects of heavy metals such as Zn^{2+} on the disturbance of Ca^{2+} homeostasis (i.e., inhibition of the activity of Ca,Mg-ATPase) due to oxidation of SH groups of the proteins. Parallel to these studies, Nasu (46) also mentioned the blockage of intracellular Ca^{2+} release in guinea-pig taenia caeci by Zn^{2+}.

All above-mentioned studies directly and/or indirectly show that there is a close relationship between an increase of $[Zn^{2+}]_i$ and an alteration of $[Ca^{2+}]_i$ handling in cardiomyocytes from diseased animals. In an interesting and supporting article by Maret (41), the cross talk of Ca^{2+} and Zn^{2+} in cellular Ca^{2+} signaling pathways was discussed in detail. Moreover, Maret and coworkers showed that intracellular Zn^{2+} fluctuations could modulate protein tyrosine phosphate activity in insulin/insulin-like growth factor-1 signaling (26).

Furthermore, it has been reported that metallothioneins (MTs) have important roles in connection with the protective function of cells by reducing damage from ROS (33). Some chemicals that stimulate the production of ROS can also increase MT levels (5, 33). Either overexpression of MT or direct MT administration could reduce diabetic cardiomyopathy and protect the cell against increased $[Zn^{2+}]_i$ toxicity via inhibiting ROS production (10, 38, 40, 63).

Moreover, the administration of trace elements and other antioxidants has been proposed as a therapeutic adjuvant in the treatment of diabetes (12, 15). Recently, Da Ros et al. (17) discussed the importance of antioxidant therapy, as well as new treatments for diabetic complications. In our previous studies, we (2, 3, 58) have also shown that treatment of streptozotocin (STZ)-induced diabetic rats with sodium selenite (5 μmol/kg) could protect the ultrastructure of the heart against diabetes-induced alterations and also restored the altered mechanical and electrical activities of the diabetic rat hearts, partially related to the restoration of the cell glutathione redox cycle.

Therefore, in the present study, from the likely involvement of oxidative stress-induced alterations in cardiac functions, our first attempt was to monitor the diabetes-induced mobilization of $[Zn^{2+}]_i$ in cardiomyocytes by using fura-2 with its relationship with the changes of levels of oxidant stress and antioxidant defense mechanisms. Our data for the first time showed that diabetic cardiomyocytes exhibited significantly increased $[Zn^{2+}]_i$ and $[Ca^{2+}]_i$, decreased levels of MT and reduced glutathione, and increased levels of lipid peroxidation (LPO) and NO products (NOPs), as well as decreased activities of superoxide dismutase, glutathione reductase (GR), and glutathione peroxidase (GPx). Treatment (4 wk) of the diabetic rats with sodium selenite (5 μmol$\cdot$kg body wt$^{-1}\cdot$day^{-1}) prevented these defects induced by diabetes. Our data indicate that oxidant stress with a shift of cell glutathione redox cycle can modulate $[Zn^{2+}]_i$ metabolism and can play important roles in oxidant-induced alterations of excitation-contraction coupling in diabetes via effecting changes in $[Ca^{2+}]_i$ in diabetic rat heart.

METHODS

Experimental Procedures

Wistar rats of both sexes (weighing 200–220 g) were housed separately according to their groups in a room with controlled temperature, humidity, and a 12-h:12-h light-dark period and received food and tap water ad libitum throughout the experiment. The rats were randomly divided into four groups. In the control group, the vehicle 0.1 M citrate buffer (pH 4.5) used to dissolve STZ was injected (0.2 ml ip) once to all rats. Some of the control group rats were treated with sodium selenite (5 μmol$\cdot$kg body wt$^{-1}\cdot$day^{-1} ip; treated control group), whereas some of them were treated with 0.1 ml volume of sodium selenite vehicle (distilled water) for 4 wk (untreated control group). Diabetes was induced by a single injection of STZ (50 mg/kg body wt ip). A week after injection of STZ, blood glucose levels were measured, and rats with blood glucose of at least three times higher than the preinjection levels were used in the experiments. Once the presence of diabetes was confirmed, diabetic rats were randomly separated into two groups: untreated diabetic group (rats injected with 0.1 ml distilled water) and treated diabetic group (rats injected with 50 mg/kg body wt sodium selenite) for 4 wk. The plasma glucose level of all animals was measured by using a glucose analyzer (Glucotrend, Roche). Plasma selenium levels were measured by using graphite-furnace atomic absorption spectrometry (AAS; AA-30/40 Varian atomic absorption spectrometer equipped with a GTA-96 Graphite Tube Atomizer, DS-15 Data Station). Plasma zinc levels were measured colorimetrically. All experimental protocols were approved by the Medical Faculty Ethics Committee on Animal Research at the Ankara University and were performed in accordance with the position of the American Heart Association on research animal use.

Isolation of Cardiomyocytes

Hearts were removed rapidly, and the aorta was cannulated on a Langendorff apparatus and then perfused retrogradely through the coronary arteries with a Ca^{2+}-free solution containing (in mM) 145 NaCl, 5 KCl, 1.2 MgSO$_4$, 1.4 Na$_2$HPO$_4$, 0.4 NaH$_2$PO$_4$, 5 HEPES, and 10 glucose at pH 7.4, bubbled with 100% O$_2$ at 37°C. Hearts were perfused for 3–5 min to be cleaned and then perfused with the same solution containing 1 mg/ml collagenase (collagenase A, Boehringer) for 30–35 min. After perfusion was completed, ventricles were removed and minced to small pieces and gently massaged through a nylon mesh, and dissociated cardiomyocytes were washed with the collagenase-free solution. The percentage of viable cells was >70% in all groups. Subsequently, Ca^{2+} in the medium was increased in a graded manner to a concentration of 1.3 mM. Cells were kept in this solution at 37°C until used in the experiments. Only these Ca^{2+}-tolerant cells were used in the experiments.

Spectrofluorometric Determinations of $[Zn^{2+}]_i$ and $[Ca^{2+}]_i$

$[Zn^{2+}]_i$ and $[Ca^{2+}]_i$ were determined in membrane-permeant fluorophore fura-2 acetoxymethyl ester (fura-2 AM)-loaded cardiomyocytes by measuring the ratio of fluorescence intensities, centered at 505 nm, in response to excitation at 340 nm and 380 nm. Loading conditions consisted of 30-min incubation of cardiomyocytes at 37°C in a HEPES-buffered solution containing 4 μM fura-2 AM. The cells were then washed twice and kept in fresh HEPES-buffered solution until use. Fura-2 fluorescence was recorded according to a method described in our previous study (57) by using a PTI Ratiomaster microspectrophotometer (Photon Technology International). Unless otherwise specified, we acquired data at a sampling rate of 60 Hz. The excitation scans were obtained for wavelengths from 320 to 400 nm, with measurements taken every nanometer for the duration of 0.5 s at each nanometer. Background fluorescence at the two different excitation wavelengths was measured before loaded cells were inserted

and was subsequently subtracted from the respective signals. Calculations of the fluorescence intensity ratios, as well as further data analysis ($[Zn^{2+}]_i$ and $[Ca^{2+}]_i$), were performed by using FELIX software (Photon Technology International).

To quantitate $[Zn^{2+}]_i$ and $[Ca^{2+}]_i$, $[Zn^{2+}]_i$ was brought to zero by the inclusion in the superfusate of 30 μM N,N,N',N'-tetrakis(2-pyridylmethyl)ethylenediamine (TPEN), a membrane-permeant Zn^{2+} chelator that does not chelate Ca^{2+}, and the residual fluorescence ratio ($F_{340/380}$) was used to determine $[Ca^{2+}]_i$. $[Zn^{2+}]_i$ was then calculated from the $F_{340/380}$ measured in the absence of TPEN.

The cardiomyocytes, placed into a small superfusion chamber mounted on the stage of the inverted microscope, were stimulated at 0.2 Hz from small platinum electrodes placed in the chamber with 20- to 30-V square pulses with 10-ms duration. Amplitude (difference between basal and peak $F_{340/380}$ ratios), time to peak (TP), and half-decay time (DT_{50}) were determined from Ca^{2+} transients evoked by field stimulation. Background fluorescence was subtracted from all recordings before the calculation of ratios.

Biochemical Assay

Sample preparation. Tissues for antioxidant enzyme section were homogenized and centrifuged at 18,000 g for 60 s at 4°C. Supernatants were collected and stored in −85°C until analysis. For other parts of the experiments, tissues were homogenized in 0.25 M sucrose solution. The homogenate was then centrifuged at 18,000 g for 20 min at 4°C. Supernatants were collected and stored at ultracold conditions. Total protein assay of homogenates was done by Lowry's method (39). All the enzyme activities for each sample were normalized per milligram of protein.

LPO. LPO assay is based on the reaction of a chromogenic reagent, N-methyl-2-phenylindole, with malondialdehyde (MDA) and 4-hyrodoxyalkenals at 45°C. One molecule of either MDA or 4-hydroxyalkenal reacts with two molecules of reagent N-methyl-2-phenylindole in acetonitrile to yield a stable chromophore with maximum absorbance at 586 nm. For simultaneous determination of MDA and 4-hydroxyalkenals, we use the procedure utilizing methanesulfonic acid as the acid solvent. The procedure in which HCl is used will only detect MDA, because the 4-hydroxyalkenals do not form a chromophore with reagent N-methyl-2-phenylindole under those conditions. With the use of the standard curve, measured activities were given (in mU/g protein).

SOD. SOD measurement is based on the SOD-mediated increase in the rate of autoxidation of 5,6,6a,11b-tetrahydro-3,9,10-rihydroxybenzo[c]fluorene in aqueous alkaline solution to yield a chromophore with maximum absorbance at 525 nm. The SOD activity is determined from the ratio of the autoxidation rates in the presence (V_s) and in the absence (V_c) of SOD. The V_s-to-V_c ratio as a function of SOD activity is independent of the type of SOD (Cu/Zn-SOD, Mn-SOD, Fe-SOD) being measured (47).

Glutathione reductase. Measurement of glutathione reductase (GR) is based on the oxidation of NADPH to $NADP^+$, catalyzed by a limiting concentration of GR. The GR-340 assay is based on the oxidation of NADPH to $NADP^+$, catalyzed by a limiting concentration of GR. One GR activity unit is defined as the amount of enzyme catalyzing the reduction of 1 μmol/min of GSSG at pH 7.6 and 25°C. One molecule of NADPH is consumed for each molecule of GSSG reduced. Therefore, the reduction of GSSG is determined indirectly by the measurement of the consumption of NADPH, as demonstrated by a decrease in absorbance at 340 nm (A_{340}) as a function of time.

Glutathione peroxidase. Glutathione peroxidase (GPx) assay is an indirect measure of the activity of cellular c-GPx (51). GSSG produced on reduction of organic peroxide by c-GPx is recycled to its reduced state by the enzyme GR. The oxidation of NADPH to $NADP^+$ is accompanied by a decrease in A_{340}, providing a spectrophotometric means for monitoring GPx enzyme activity. The molar

extinction coefficient for NADPH is 6,220 $M^{-1} \cdot cm^{-1}$ at 340 nm. To assay c-GPx, a cell or tissue homogenate is added to a solution containing glutathione, GR, and NADPH. The enzyme reaction is initiated by adding the substrate *tert*-butyl hydroperoxide, and the A_{340} is recorded. The rate of decrease in the A_{340} is directly proportional to the GPx activity in the sample.

Total glutathione. Measurement of total glutathione is based on a chemical reaction, which proceeds in two steps. The first step leads to the formation of substitution products (thioethers) between a patented reagent, 4-chloro-1-methyl-7-trifluromethyl-quinolinium methylsulfate (R1), and all mercaptans (RSH) that are present in the sample. The second step is β-elimination reaction, which takes place under alkaline conditions. This reaction is mediated by reagent NaOH (30%, R2), which specifically transforms the substitution product (thioether) obtained with GSH into a chromophoric thione, which has a maximal absorbance wavelength at 400 nm.

GSH. Measurement of GSH is based on the formation of a chromophoric thione (French Patent No. 9115868; United States Patent No. 5,817,520). The absorbance measured at 420 nm is directly proportional to the GSH concentration. There are three steps to the reaction. First, the sample is buffered, and the reducing agent tris(2-carboxyethyl)phosphine is added to reduce any GSSG to the reduced state. The chromogen R1 is added, forming thioethers with all thiols present in the sample. With the addition of base raising the pH >13, a β-elimination specific to the GSH-thioether results in the chromophoric thione. The amount of GSSG is calculated by subtracting the measured GSH from the measured total glutathione.

NOPs. Measurement of NOPs is based on the determination of nitrite. Spectrophotometric determination of nitrite using Greiss reagent is straightforward and sensitive but does not measure nitrate, causing a possible underestimation of NO. To eliminate the underestimation, granular cadmium metal for chemical reduction of nitrate to nitrite was done. In acid solution, nitrite is converted to nitrous acid (HNO_2), which diazotizes sulfanilamide. This sulfanilamide-diazonium salt is then reacted with N-(1-naphthyl)-ethylenediamine to produce a chromophore, which is measured at 540 nm.

MT. Determination of MT is made by Ag saturation method. The amount of Ag^+ in the supernatants was estimated by using Z-8200 Hitachi flame AAS (53). Briefly, the estimation of MTs by the Ag^+ saturation method exploits the high Ag^+-binding capacity and heat stability of MTs. The amount of Ag^+ in the final supernatant fraction is proportional to the amount of MTs present. In addition to that, MT can potentially bind to 20 mol Ag^+/mol protein. Calculations of MT protein were done by 1 μg Ag^+ representing 3.55 μg MT.

Chemicals and Statistical Evaluation of Data

All chemicals used were purchased from Sigma (Sigma-Aldrich Chemie, Steinheim, Germany), except for fura-2 AM, which was purchased from Molecular Probes (Eugene, OR), and collagenase A, which was purchased from Boehringer Mannheim (Roche Diagnostics, Mannheim, Germany). Two groups were compared with Student's *t*-test. $P < 0.05$ was taken as significant. Data are means ± SE.

RESULTS

General Characteristics of Animals

Sodium selenite treatment significantly affected weight gain only in the treated diabetics compared with the untreated diabetics (Fig. 1). The average body weight was significantly lower in diabetic rats compared with that in the control rats at 5 wk after STZ injection (Table 1). Moreover, sodium selenite treatment could prevent deleterious weight loss seen in untreated diabetic rats. Sodium selenite treatment caused a small but significant increase in blood glucose level ($P < 0.05$ vs.
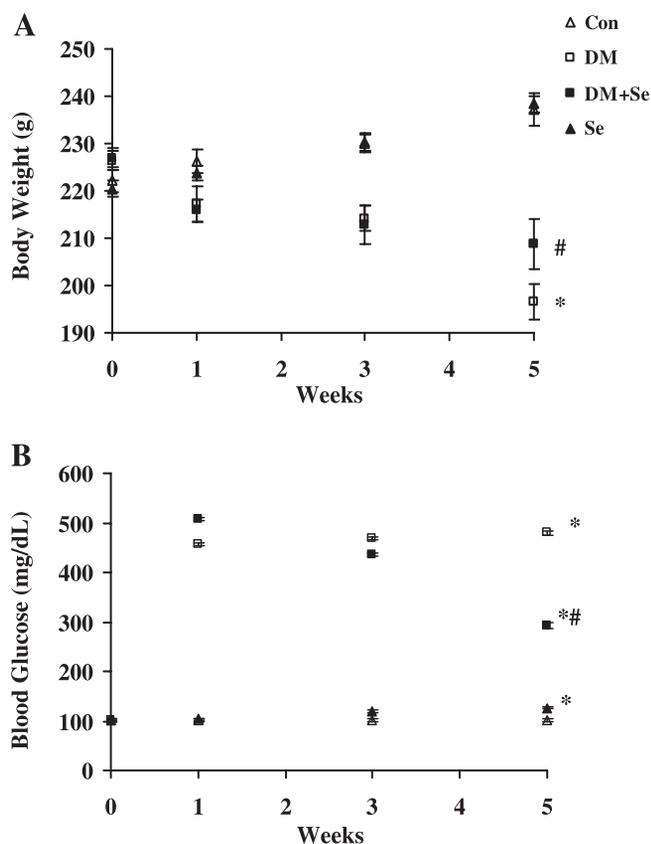
Fig. 1. Time courses of body weights (*A*) and blood glucose levels (*B*) of groups for 5 wk. Value are means ± SE of rats used in the experiments. Zero represents day before streptozotocin (STZ) or vehicle injection, whereas 1–4 are the weeks after STZ injection. Untreated control group (Con) were normal rats injected with single dose of citrate buffer. Untreated diabetic group (DM) were rats with single dose of STZ injection. Treated diabetic group (DM + Se) were rats treated with sodium selenite for 4 wk starting 1 wk after single dose of STZ injection. Treated control group (Se) were rats treated with sodium selenite for 4 wk starting 1 wk after single dose of citrate buffer injection. Student's *t*-test was used. *$P < 0.001$ vs. untreated control group; #$P < 0.01$ vs. untreated diabetic group.

untreated control group). Treatment of the diabetic animals with sodium selenite did decrease high blood glucose level with a small but significant ($P < 0.05$) level compared with that in the untreated diabetic group.

After the first week of STZ injection, 24% of diabetic rats died during the 4-wk experimental period and 20% from the sodium selenite-treated diabetic group. On the other hand, there was no loss in numbers from either untreated or treated control groups. Neither diabetes nor 4 wk of sodium selenite treatment of these rats could significantly induce any change in both plasma selenium and zinc levels (Table 1).

Measurement of [Zn^{2+}]$_i$ in Cardiomyocytes

To quantitate [Zn^{2+}]$_i$, we followed the procedure that was published previously (57). Briefly, apparent dissociation constants were determined by in vitro experiments while minimum and maximum fluorescence ratios (R$_{min}$ and R$_{max}$, respectively) were measured directly from fura-2-loaded cardiomyocytes (57). The apparent dissociation constants used here were 1.3 and 330 nM for Zn^{2+} and Ca^{2+}, respectively. As observed by others (59), the excitation spectra demonstrated a shift of

the isosbestic wavelength from 361 nm in the presence of Ca^{2+} to 374 nm in the presence of Zn^{2+} (data not shown). In the physiological pCa range, the addition of as little as 10 nM Zn^{2+} had a substantial inhibitory effect on the fura-2 response to Ca^{2+} as expected from the ~250-fold higher affinity of fura-2 for Zn^{2+} than for Ca^{2+} (59).

We determined intracellular R$_{min}$ and R$_{max,Zn}$ values using the protocol illustrated in Fig. 2*A*. For R$_{max,Zn}$, the myocytes were exposed to the zinc ionophore Zn-pyrithione (1 μM). The resulting increase in F$_{340/380}$ reached a steady-state maximum value of 1.07 ± 0.01 ($n = 19$ rats) after 5 min, representing the highest ratio that can be elicited by saturating concentrations of intracellular free Zn^{2+} (Fig. 2*A*, *right*). The assumption that 1 μM Zn-pyrithione was sufficient to elevate [Zn^{2+}]$_i$ to saturating levels is supported by our previous observations (57). The addition of the membrane-permeant Zn^{2+} chelator TPEN (30 μM) caused a rapid decrease of fluorescence ratio to a level lower (0.34 ± 0.01) than that measured under control conditions (0.43 ± 0.01), verifying that the increased ratio was attributable to zinc.

Sodium Selenite Treatment of Diabetic Rats Prevents Increases of Basal [Zn^{2+}]$_i$ and [Ca^{2+}]$_i$ of Cardiomyocytes

As shown from Fig. 2, *B–D*, the average [Zn^{2+}]$_i$ and [Ca^{2+}]$_i$ values of diabetic rat cardiomyocytes are 0.87 ± 0.05 nM and 49.66 ± 9.03 nM, respectively, and significantly higher than the respective control values (0.52 ± 0.06 nM and 26.53 ± 3.67 nM, respectively). Sodium selenite treatment (4 wk) of the diabetic rats caused a significant normalization of these values to the control values. As seen from Fig. 2, these values for [Zn^{2+}]$_i$ and [Ca^{2+}]$_i$ are 0.69 ± 0.05 nM and 23.67 ± 4.34 nM (Fig. 2*C*), respectively. The treatment of the normal rats with the same amount of sodium selenite for the same period has no significant effects on these parameters (0.57 ± 0.04 nM and 24.27 ± 3.78 nM for [Zn^{2+}]$_i$ and [Ca^{2+}]$_i$, respectively).

The measurement of R$_{min}$ necessitated the hyperpermeabilization of the cell membrane to wash out all intracellular

Table 1. *Characteristics of control and diabetic rats with or without sodium selenite treatment*

Groups	Body Weight, g	Blood Glucose, mg/dl	Plasma Se, ng/ml	Plasma Zn, μg/dl
Control groups				
Untreated	235.2±1.8	101.8±0.5	113.85±0.5	191.5±26.8
n	19	19	9	9
Treated	234.9±2.1	129.2±3.5*	126.7±5.8	198.7±15.8
n	19	19	10	10
Diabetic groups				
Untreated	203.0±3.6*	469.2±10.7*	107.1±10.8	201.1±11.7
n	23	23	9	9
Treated	226.5±1.8	333.5±15.5*†	138.3±8.8	213.3±18.9
n	18	18	8	8

Values are means ± SE; *n*, number of animals. Control groups, rats with a single dose of citrate buffer-injected injection; diabetic groups, rats with a single dose of streptozotocin injection; treated subgroups, rats treated with sodium selenite for 4 wk starting 1 wk after single dose of streptozotocin or citrate buffer injection; Se and Zn, plasma selenium and zinc levels of groups, respectively. Student's *t*-test was used. *$P < 0.001$ vs. untreated control group; †$P < 0.01$ vs. untreated diabetic group.
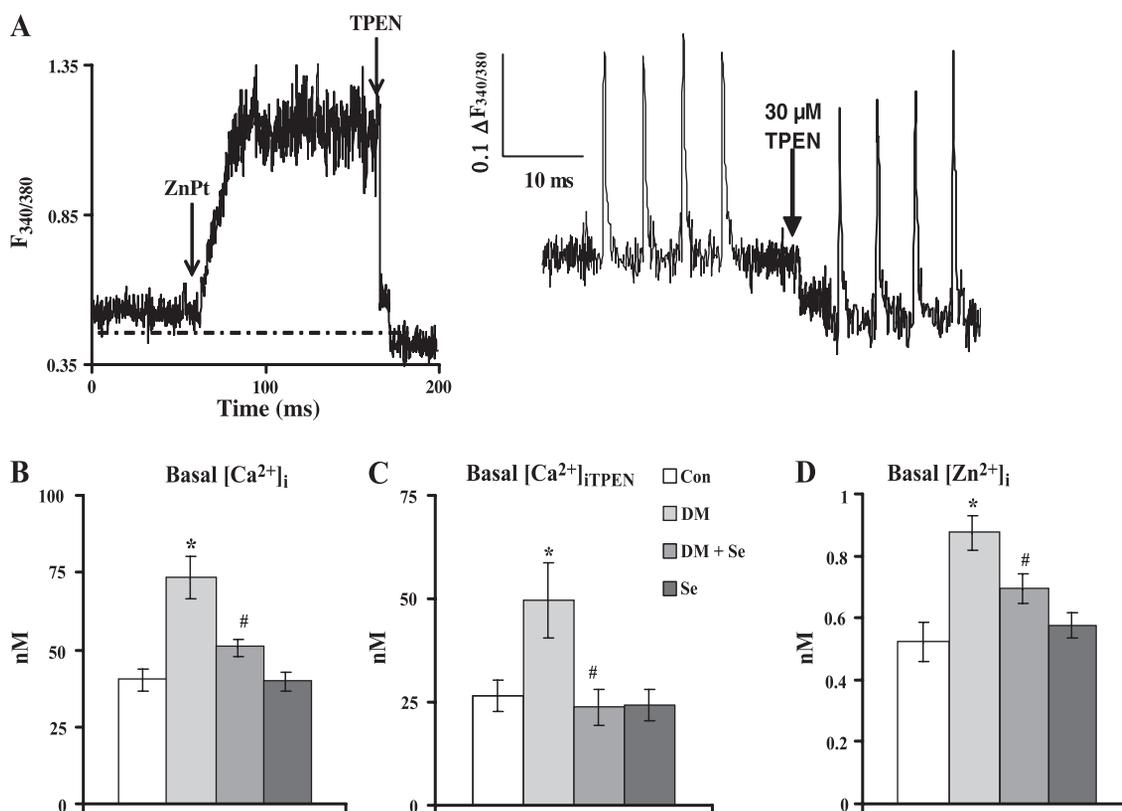
Fig. 2. Determination of intracellular minimum and maximum fluorescence ratio ($F_{340/380}$) values for Zn^{2+}. *A*: isolated cardiomyocytes were first superfused with HEPES-buffered solution containing 0.1 mM $CaCl_2$ and then perfused with 1.8 mM $CaCl_2$ containing 2 mM EGTA for 2 min. No change in $F_{340/380}$ was observed during that time. Cells were then exposed at indicated times (arrows) to 1 μM zinc-pyrithione (ZnPT), followed by 30 μM N,N,N',N'-tetrakis(2-pyridylmethyl)ethylenediamine (TPEN) in same superfusate. As indicated by dashed lines, exposure to TPEN caused decrease of $F_{340/380}$ to below basal level (*left*). To test possibility of Zn^{2+} transients under electric field stimulation, we exposed cells to TPEN and continued to record fluorescence changes by inducing 20- to 30-V pulses application with 10-ms duration at 0.2-Hz frequencies (*right*). *B*: basal values are means ± SE of intracellular calcium concentration ($[Ca^{2+}]_i$) without TPEN. *C*: $[Ca^{2+}]_i$ with TPEN ($[Ca^{2+}]_{iTPEN}$). *D*: intracellular zinc concentration ($[Zn^{2+}]_i$) with TPEN. Specifications of groups are given in Fig. 1. Student's *t*-test was used. *$P < 0.05$ vs. untreated control group; #$P < 0.05$ vs. untreated diabetic group.

Zn^{2+} and Ca^{2+}. Exposure of fura-2-loaded cells to membrane-permeabilizing digitonin, in combination with EGTA and the heavy metal chelator nitrilotriacetic acid (NTA), decreased the basal $F_{340/380}$ by 20–40% to a steady-state minimum level of 0.25 ± 0.01 ($n = 8$), confirming that the membrane became permeable to the ion chelators (data not shown).

In summary, the values utilized for the determination of $[Zn^{2+}]_i$ and $[Ca^{2+}]_i$ using the equation mentioned in our previous publication (57) are 1.79 nM and 3.75 μM for the apparent dissociation constants of Zn^{2+} and Ca^{2+}, 1.07 and 2.2 for $R_{max,Zn}$ and $R_{max,Ca}$, and 0.25 for R_{min}. As shown in the Fig. 2*A*, exposure to TPEN (either with Zn-pyrithione exposure or electric-field stimulation) caused a decrease of the $F_{340/380}$ below basal levels, indicating the presence of measurable intracellular free Zn^{2+} levels. Figure 2*D* could give the computed values measured from cells exposed to TPEN only (i.e., without pyrithione treatment). As shown in the bar graphs, the highly significant TPEN-induced decrease in $F_{340/380}$ from 0.43 to 0.34 indicated an average $[Zn^{2+}]_i$ value of 0.52 ± 0.06 nM. This resulted in a calculated $[Ca^{2+}]_i$ value of 26.54 ± 3.67 nM instead of the apparent 40.17 ± 3.73 nM that would have been estimated in the absence of the confounding Zn^{2+} effect (Fig. 2*C*).

Effect of Sodium Selenite Treatment and Diabetes on Ca^{2+} Transients

The effects of sodium selenite treatment of rats and diabetes in the presence of normal extracellular Ca^{2+} (1.8 mM) on electrically field-stimulated cardiomyocytes were also examined. Figure 3 illustrates the effect of diabetes and sodium selenite treatment of both diabetic and control rats on $F_{340/380}$ values recorded from cardiomyocytes superfused with 1.8 mM Ca^{2+} and stimulated under field effect without TPEN exposure. As can be seen from the original traces in Fig. 3*A*, the amplitude and kinetic parameters of the traces from diabetic cardiomyocytes are significantly different from the controls. These two traces are put together in the same scale for comparison. The average value of the amplitude of Ca^{2+} transients recorded from diabetic rat cardiomyocytes is significantly smaller than the control (Fig. 3*C*). Both TP (Fig. 3*B*) and DT_{50} (Fig. 3*D*) of Ca^{2+} transients of cardiomyocytes isolated from diabetic rats are significantly slower than those from control rats. As can be seen from the bar graphs, sodium selenite treatment of diabetic rats can cause a complete restoration in the amplitude and a significant effect on prolonged DT_{50} but no significant effect on prolonged TP. On the other hand, sodium selenite treatment (4 wk) of the
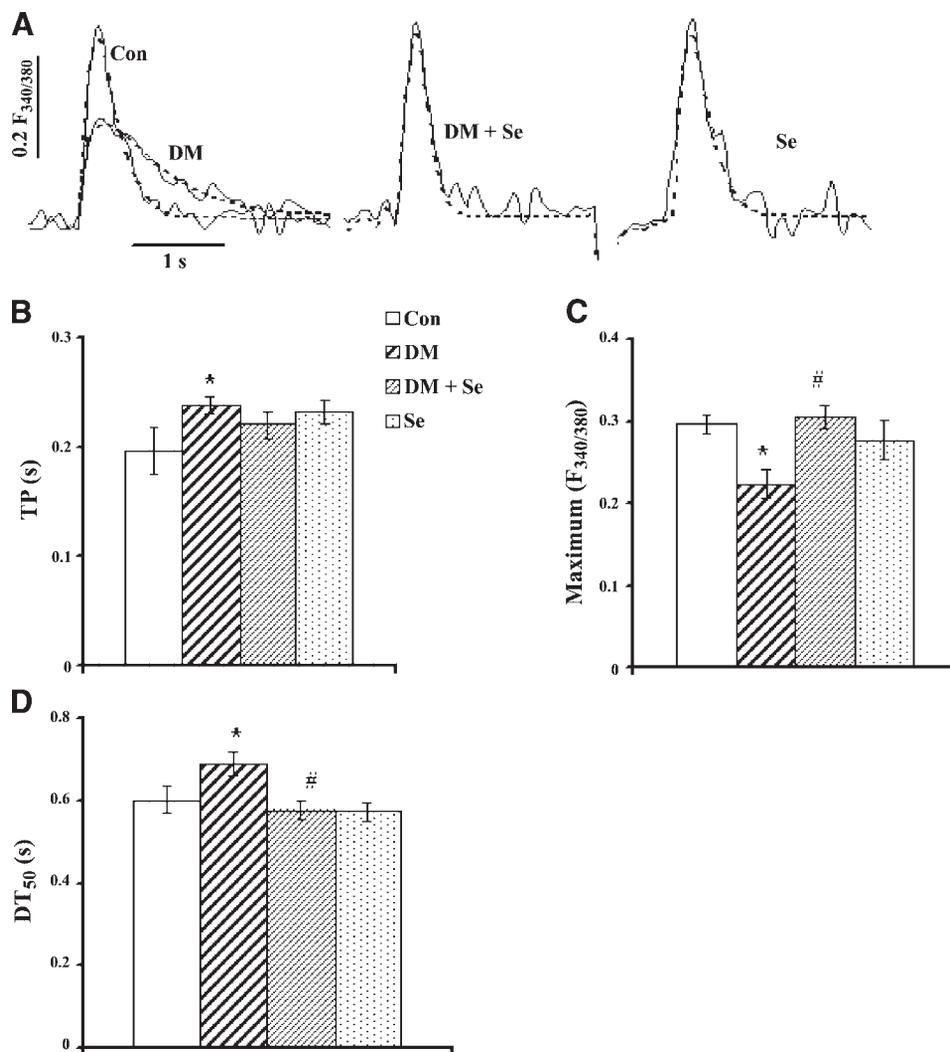
Fig. 3. Effect of sodium selenite on intracellular Ca^{2+} transients. *A*: representative intracellular Ca^{2+} transient traces of isolated cardiomyocytes from Con, Se, DM, and DM + Se without considering intracellular Zn^{2+}. Transients were induced by application of 20- to 30-V pulses with 10-ms duration at 0.2-Hz frequencies. Kinetic parameter values are means ± SE of Ca^{2+} transients of isolated cardiomyocytes from 4 groups. *B*: TP, time to peak (maximum). *C*: maximum $\Delta F_{340/380}$, peak $F_{340/380}$ − basal $F_{340/380}$. *D*: DT_{50}, decay time to 50% of peak. Values are means ± SE of 27–60 cells from at least 5 animals. Student's *t*-test was used. *$P < 0.05$ vs. untreated control group; #$P < 0.05$ vs. untreated diabetic group.

control rats has no significant effects on these measured parameters.

To be able to test a possible interference of Zn^{2+} transients under field stimulation, we exposed the cells to TPEN and then measured all the parameters of Ca^{2+} transients mentioned in METHODS. The average values were put in Table 2. As can be seen from these data (compared with the data in Fig. 3), there are no Zn^{2+} transients under field stimulation (Fig. 3*A*, *left*); the transient data arise only from Ca^{2+} transients without any interference with Zn^{2+} transients. These sets of experiments demonstrated that Zn^{2+} could mobilize from associated proteins in diabetes chronically but not transiently, most probably, via oxidative stress during a long period, and there is no transient Zn^{2+} release from cardiomyocytes under electric-field stimulation either in control or in diabetic states.

Effect of Sodium Selenite Treatment on Diabetes-Induced Oxidant Stress in Heart

MDA content, which is indicative of LPO, increased significantly in the diabetic rat heart with respect to the control group. Sodium selenite treatment of the rats caused a complete normalization in the diabetic group, whereas there was no effect in the control group (Fig. 4*A*). We also measured NOPs, which are indicative of oxidant stress in the cell. NOP levels

increased significantly in diabetic rat heart tissue, and sodium selenite treatment of these diabetic rats prevented this increase significantly, whereas there was no significant effect on the control rats (Fig. 4*B*).

Table 2. *Parameters of intracellular Ca^{2+} transients exposed to TPEN*

Parameters	TP, s	MA, $\Delta F_{340/380}$	DT_{50}, s
Control groups			
Untreated	0.18±0.02	0.27±0.03	0.57±0.03
Treated	0.23±0.01	0.27±0.01	0.55±0.02
Diabetic groups			
Untreated	0.22±0.01*	0.22±0.02*	0.67±0.04*
Treated	0.21±0.02†	0.31±0.02†	0.52±0.03†

Values are means ± SE of 27–60 cells from at least 5 animals. Cells exposed to *N,N,N′,N′*-tetrakis(2-pyridylmethyl)ethylenediamine (TPEN) and continued to record fluorescence changes by inducing 20- to 30-V pulses with 10-ms duration at 0.2 Hz. Mean kinetic parameters of Ca^{2+} transients of isolated cardiomyocytes from control and diabetic rats are given. MA, maximum amplitude ($\Delta F_{340/380}$ = $F_{340/380}$ peak − $F_{340/380}$ basal); TP, time to peak (maximum); DT_{50}, decay time to 50% of peak. Specifications of groups are given in Table 1. Student's *t*-test was used. *$P < 0.05$ vs. untreated control group; †$P < 0.05$ vs. untreated diabetic group.
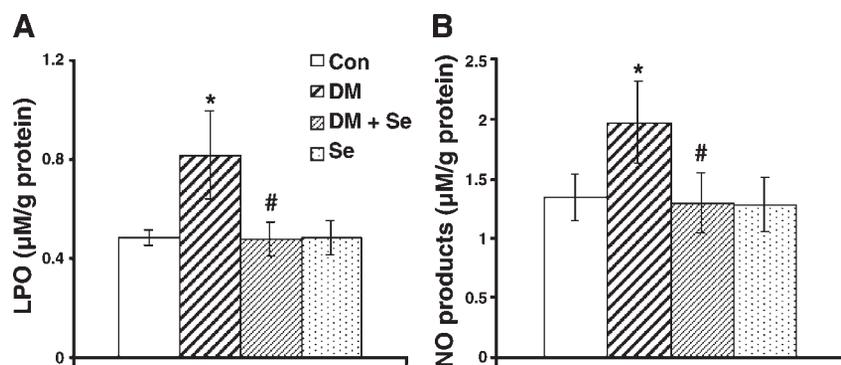
A

B

Fig. 4. Effect of sodium selenite on levels of oxidants in heart tissues. Levels of lipid peroxidation (LPO; *A*) and nitric oxide (NO) products (*B*) are significantly normalized with selenium treatment of diabetic rats for 4 wk. Values are means ± SE of 7 rats. Specifications of groups are given in Fig. 1. Student's *t*-test was used. *$P < 0.001$ vs. untreated control group; #$P < 0.01$ vs. untreated diabetic group.

Both SOD and GR activities are depressed significantly in the diabetic rat hearts, whereas GPx activity increased. These three different enzyme activities, which play important roles in the antioxidant defense system in the cell, were normalized with sodium selenite treatment (Fig. 5, *A–C*, respectively).

Diabetes induced a significant reduction in GSH and an increase in GSSG contents in cardiac tissue with respect to the control group (Table 3). Treatment of the diabetic rats with sodium selenite (4 wk) caused a significant attenuation in the GSH-to-GSSG ratio, which is a good estimation of the redox state as well as oxidative stress. The treatment of the rats from the control group with the same amount of sodium selenite surprisingly has a small but significant effect on this ratio (Table 3).

Effect of Sodium Selenite Treatment on Heart MT Level

We measured in heart tissue an antioxidant protein MT level, which is a cysteine-rich protein, can bind heavy ion such

as zinc, and has a strong effect in scavenging free radicals. As can be seen from Table 3, diabetes can induce a significant decrease in MT levels, and sodium selenite treatment of the diabetic rats can prevent this decrease and normalize to the control level. The treatment of the normal rats with sodium selenite has no significant effect on MT level of the heart tissue.

DISCUSSION

One of the major findings of the present study is that diabetes induced a significant increase in basal $[Zn^{2+}]_i$ parallel to the increased basal $[Ca^{2+}]_i$. This is the first study to evaluate both $[Zn^{2+}]_i$ and $[Ca^{2+}]_i$ of cardiomyocytes from diabetic rats quantitatively and comparatively. These are the first important data that demonstrate the beneficial effect of the antioxidant sodium selenite on intracellular Ca^{2+} metabolism of diabetic rat heart. Previous studies from our laboratory (2, 3) have already demonstrated that sodium selenite treatment (4 wk) of diabetic rats has beneficial effects on both mechanical and
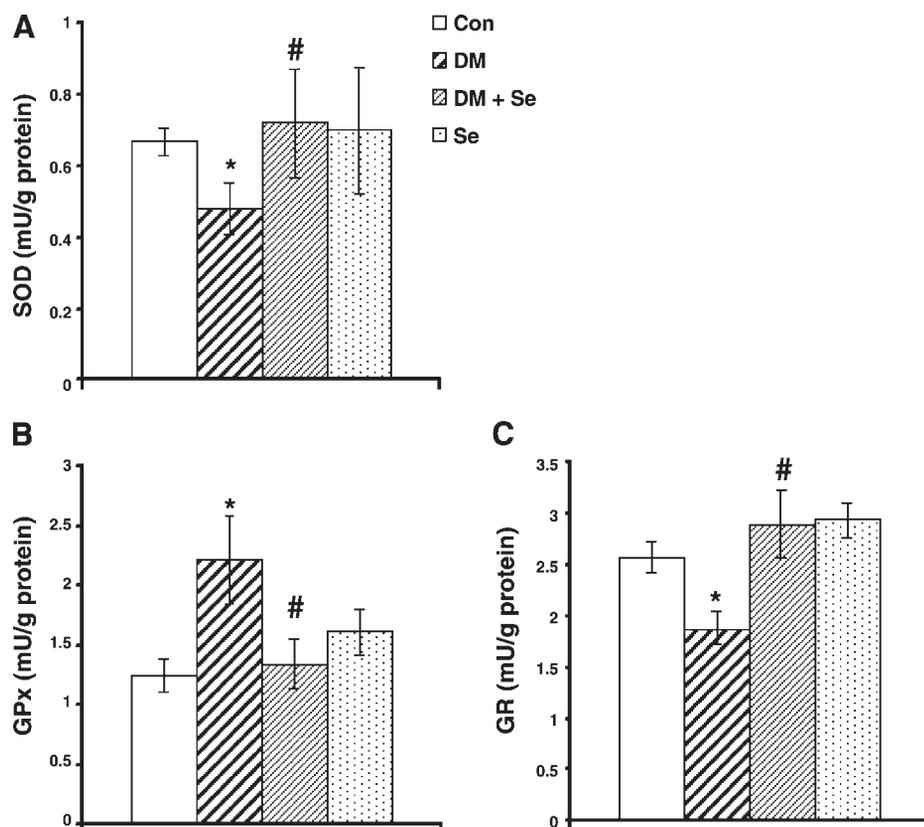
A

B

C

Fig. 5. Effect of sodium selenite on activities of antioxidants in heart tissues. Activities of superoxide dismutase (*A*), glutathione peroxidase (GPx; *B*), and glutathione reductase (GR, *C*) are significantly normalized with selenium treatment of diabetic rats for 4 wk. Values are means ± SE of 7 rats. Specifications of groups are given in Fig. 1. Student's *t*-test was used. *$P < 0.001$ vs. untreated control group; #$P < 0.01$ vs. untreated diabetic group.

Table 3. *Effects of selenium treatment on biochemical parameters of control and diabetic rats*

Groups	n	GSH, μM/g tissue	GSSG, μM/g tissue	GSH/GSSG	MT, μg/g tissue
		Control groups			
Untreated	8	68.2±0.4	3.2±1.0	21.5±3.5	39.0±1.8
Treated	7	59.7±0.3	5.4±0.9*	11.1±3.4*	37.7±6.9
		Diabetic groups			
Untreated	8	47.6±1.2*	8.7±1.7*	5.5±1.8*	24.4±4.0*
Treated	8	57.1±4.1	5.2±1.4*	11.1±2.9†	43.2±7.0

Values are means ± SE; *n,* number of animals. MT, metallothionien. Specifications of groups are given in Table 1. Student's *t*-test was used. *$P <$ 0.001 vs. untreated control group; †$P <$ 0.01 vs. untreated diabetic group.

electrical activities due to a restoration of inhibited K^+ currents via an effect in cell glutathione redox cycle. Therefore, the present data can be considered as strong evidence of the roles of increased basal $[Zn^{2+}]_i$ in altered contractile activity due to alteration of $[Ca^{2+}]_i$ metabolisms. Second, the data can emphasize the involvement of oxidant stress in the etiology of diabetes-induced cardiac dysfunction due to alteration of cellular Ca^{2+} handling and the close relationship between insulin deficiency, or impaired insulin signaling, and alteration in contractile activity of diabetic heart via depressed endogenous antioxidant defense mechanism.

Oxidants Greatly Increase Basal $[Zn^{2+}]_i$

The present study showed that diabetes induced a significant increase in basal $[Zn^{2+}]_i$. Our biochemical data also support that this increase, as well as an increase in basal $[Ca^{2+}]_i$, together with alterations in the parameters of $[Ca^{2+}]_i$ transients, can be attributed mostly due to increased ROS production in cardiomyocytes. Together with the other researches, we have demonstrated that $[Zn^{2+}]_i$ could also increase rapidly in cardiomyocytes and endothelial cells as a result of the mobilization of Zn^{2+} from intracellular stores by ROS (36, 40, 42, 56). All these studies demonstrate a close relationship between an increase and the deleterious effects of $[Zn^{2+}]_i$ and oxidant stress under diseased states of the heart. Furthermore, Bossy-Wetzel et al. (8) have discussed the cross talk between NO and Zn^{2+} pathway to cell death due to formation of peroxynitrite and consequent Zn^{2+} release from intracellular stores. These data also imply the contribution and importance of distribution of $[Zn^{2+}]_i$ due to increased oxidative and nitrosative stress in diabetic rat heart.

Cardiac dysfunction is an important component of the adverse effects of diabetes. Depression in contractile activity of diabetic rats paralleled the reduced rise and decline rates of $[Ca^{2+}]_i$ transients (14). This study reports significant alterations in Ca^{2+} homeostasis that can account for the well-known contractile dysfunction in such pathological conditions. In the present study, we first confirmed the defective intracellular Ca^{2+} signaling with both lower amplitude and slower kinetics of Ca^{2+} transients. Furthermore, we clearly established that increased basal $[Zn^{2+}]_i$ might have an important contribution to defects in contractile activity. In addition, the present data showed that diabetes could induce and/or cause oxidant stress, and, therefore, mobilization of Zn^{2+} from intracellular stores might contribute to oxidant-induced alter-

ations of excitation-contraction coupling in diabetic rat heart. This hypothesis is supported by previously published data (3). It is highly likely that $[Zn^{2+}]_i$ or any mechanism that alters its concentration and distribution will cause profound functional effects in cardiomyocytes.

MT and Increased Basal $[Zn^{2+}]_i$

Our data showed that MT level of diabetic rat heart is significantly reduced, whereas basal $[Zn^{2+}]_i$ increased and the plasma Zn^{2+} level did not change significantly. It has been reported that MT level has important roles in connection with the protective function to cells by reducing damage from ROS (33). Furthermore, it has been demonstrated that either over-expression of MT or direct MT administration could reduce diabetic cardiomyopathy and protect the cell against increased $[Zn^{2+}]_i$ toxicity via inhibiting ROS production (10, 40, 38, 63). In addition, this very likely supports a close relationship between an increase of $[Zn^{2+}]_i$ and alteration of $[Ca^{2+}]_i$ in cardiomyocytes from diseased animals (29). Related with the above hypothesis, the study by Maret (41) also discussed in detail a cross talk of Ca^{2+} and Zn^{2+} in cellular Ca^{2+} signaling pathways. In addition, modulation of protein tyrosine phosphates activity with intracellular Zn^{2+} fluctuations has been shown in insulin/insulin-like growth factor-1 signaling (26).

Several studies (13, 19, 29, 45, 46, 61) support the role and importance of the changes of $[Zn^{2+}]_i$ in Ca^{2+} metabolisms and contractile activity of the heart. Recent studies (13, 45, 61) demonstrated inhibition of intracellular Ca^{2+} release mechanisms by Zn^{2+} and discussed the cytotoxic effects of Zn^{2+} on the disturbance of Ca^{2+} homeostasis due to oxidation of SH groups of the proteins (60). Therefore, involvement of oxidant stress in the etiology of diabetes-induced increase of basal $[Zn^{2+}]_i$ and alterations of $[Ca^{2+}]_i$ metabolism is confirmed by our data.

MT is a potent antioxidant enzyme and binds seven Zn^{2+} with sulfur ligands (33), and redox reagents are asymmetrically involved in both directions of Zn^{2+} transfer from enzymes to thionein (25, 31). GSH mediates Zn^{2+} transfer from enzymes to thionein, whereas glutathione disulfide oxidizes MT with an enhanced release of Zn^{2+} and transfer of Zn^{2+} to apoenzymes (25, 31). This pathway seems true for our model due to the increased GSSG and MT and the decreased GSH. Recent studies (33, 64) demonstrated also that the controlled level of MT is very important for the normal function of the organs under disease states. Moreover, it is very important to consider the toxic side of the possible increase of $[Zn^{2+}]_i$, which can cause dysfunctions in cell systems even if in the level of gene expression and apoptosis (1, 35). Therefore, our present data point out the importance of the defense mechanisms of the heart in diabetes.

Beneficial Effect of Selenium on Increased Basal $[Zn^{2+}]_i$ and $[Ca^{2+}]_i$

We observed significantly increased $[Zn^{2+}]_i$ and $[Ca^{2+}]_i$, depressed antioxidant defense system together with depressed MT level in diabetic rat hearts. Sodium selenite treatment of the diabetic rats could profoundly protect the diabetic heart against functional dysfunction (3) due to its antioxidant role in this defense system together with its other important roles in intracellular metabolic pathways, including MAP kinases, that are normally activated with insulin (28, 54).

Alterations of antioxidant enzymes SOD, GPx, and GR and increases of LPO, GSSG, and NOPs support the idea of altered Ca^{2+} metabolisms in the heart due to increased oxidant stress in diabetes. In addition, a significant increase of $[Zn^{2+}]_i$ and a decrease of MT level also support the above idea. Treatment of these animals with sodium selenite could normalize almost all these altered parameters that are parallel with previously published data (7, 24, 44). Once more, our data strongly show the alteration of Ca^{2+} metabolisms due to increased oxidant stress and depressed antioxidant defense mechanism and, moreover, the increase of $[Zn^{2+}]_i$ due to mobilization of Zn^{2+} from intracellular stores. Although there are no direct data, several studies (1, 13, 19, 29, 45, 46, 60, 61) discussed in detail the roles of increased $[Zn^{2+}]_i$ in cell functions due to oxidation of SH groups by Zn^{2+} and/or cytotoxic effects of Zn^{2+} in $[Ca^{2+}]_i$ metabolisms. All these studies demonstrate the close relationship between the increase of $[Zn^{2+}]_i$ and the alteration of $[Ca^{2+}]_i$ metabolisms in cardiomyocytes from diseased animals as well as altered insulin pathways (26, 41). Moreover, the importance of antioxidant therapy in subcellular remodeling and heart dysfunction in diabetes is emphasized in review articles (17, 18). Schaffer et al. (52) also showed a normalization of enhanced platelet Ca^{2+} response in diabetics by an antioxidant glutathione and demonstrated that this alteration in Ca^{2+} signaling by diabetes was due to increased formation of superoxide anions and reduced NO production.

Is the Beneficial Effect of Selenium Due to Its Insulin Mimetic Effect in STZ-Induced Diabetic Rats?

The mechanisms of sodium selenite-mediated normalization of altered mechanical and electrical activities of diabetic rat heart are not fully understood at this time. However, our hypothesis of antioxidant effect via glutathione involvement is supported by recent studies (6, 9, 17, 18, 37, 43, 62, 63). These studies demonstrated that exogenous application of glutathione and other antioxidants, such as SOD, catalase, or their mimetic compounds, protected the heart of diabetic rats via insulin-signaling cascade. Therefore, it is quite tempting to suggest the possible roles of this signaling pathway in controlling the intracellular redox state and the normal function of cardiac myocytes. Therefore, previously published data offer further insight into the mechanisms at play in this model. Under in vitro conditions, it has been shown that sodium selenate treatment of adiposities could increase glucose uptake and phosphorylation, as well as the activity of several signaling proteins that are normally activated with insulin (20, 28, 54). Thus, when evaluating the published data with the present findings, it seems likely that sodium selenite treatment affects the diabetes-induced heart dysfunction through its effect on cell GSH, which, in turn, is closely related with the insulin-signaling cascade.

Moreover, sodium selenite administration to the normal rats caused a slight but significant increase in blood glucose level and a significant decrease in plasma insulin level. Previously, we (4) have also shown some important alterations in the kinetics of Ca^{2+} and K^+ currents due to the effect of selenium on insulin-signaling cascade via alterations in the cell redox status. Although there are no direct data, some authors (22, 34, 37) showed that either external or internal application of GSSG leads to changes in ionic channels and is related to altered GSSG levels and coupled to insulin-signaling cascade. There-

fore, under these implications, our data showed that sodium selenite can affect some functions of normal rats via a change in cellular GSH level due to increased blood glucose level and decreased plasma insulin level. Additional studies are needed to determine whether small doses of selenium compounds may be useful and/or prooxidant when used as supplements in normal human diets.

In conclusion, all the above observations demonstrate the current controversies on this subject, but it is clear that the impaired contractility of intact diabetic hearts can be due to defects in cellular Ca^{2+} metabolisms of an individual cardiomyocyte. It can be concluded that there is a lack of complete clarification in the molecular mechanisms of cardiac dysfunction in diabetes, for which further studies are needed.

REFERENCES

1. **Atar D, Backx PH, Appel MM, Gao WD, and Marban E.** Excitation-transcription coupling mediated by zinc influx through voltage-dependent calcium channels. *J Biol Chem* 270: 2473–2477, 1995.
2. **Ayaz M, Can B, Ozdemir S, and Turan B.** Protective effect of selenium treatment on diabetes-induced myocardial structural alterations. *Biol Trace Elem Res* 89: 215–226, 2002.
3. **Ayaz M, Ozdemir S, Ugur M, Vassort G, and Turan B.** Effects of selenium on altered mechanical and electrical cardiac activities of diabetic rat. *Arch Biochem Biophys* 426: 83–90, 2004.
4. **Ayaz M, Ozdemir S, Yaras N, Vassort G, and Turan B.** Selenium-induced alterations in ionic currents of rat cardiomyocytes. *Biochem Biophys Res Commun* 327: 163–173, 2005.
5. **Banman JW, Liu J, Liu YP, and Klaassen CD.** Increase in metallothionein produced by chemicals that induce oxidative stress. *Toxicol Appl Pharmacol* 110: 347–354, 1991.
6. **Beckman JA, Goldfine AB, Gordon MB, and Creager MA.** Ascorbate restores endothelium-dependent vasodilation impaired by acute hyperglycemia in humans. *Circulation* 103: 1618–1623, 2001.
7. **Berg EA, Wu JY, Campbell L, Kagey M, and Stapleton SR.** Insulin-like effects of vanadate and selenate on the expression of glucose-6-phosphate dehydrogenase and fatty acid synthase in diabetic rats. *Biochimie* 77: 919–924, 1995.
8. **Bossy-Wetzel E, Talantova MV, Lee WD, Scholzke MN, Harrop A, Mathews E, Gotz T, Han J, Ellisman MH, Perkins GA, and Lipton SA.** Crosstalk between nitric oxide and zinc pathways to neuronal cell death involving mitochondrial dysfunction and p-38-activated K^+ channels. *Neuron* 41: 351–365, 2004.
9. **Brownlee M.** Biochemistry and molecular cell biology of diabetic complications. *Nature* 414: 813–820, 2001.
10. **Cai L, Wang j Li Y, Wang L, Zhou Z, and Kang YJ.** Inhibition of superoxide generation and associated nitrosative damage is involved in metallothionein prevention of diabetic cardiomyopathy. *Diabetes* 54: 1829–1837, 2005.
11. **Ceriello A, Dello Russo P, Amstad P, and Cerutti P.** High glucose induces antioxidant enzymes in human endothelial cells in culture. Evidence linking hyperglycemia and oxidative stress. *Diabetes* 45: 471–477, 1996.
12. **Ceriello A.** New insights on oxidative stress and diabetic complications may lead to a "causal" antioxidant therapy. *Diabetes Care* 26: 1589–1596, 2003.
13. **Cheng XY, Chen KY, Zhang XH, and Zhu PH.** Effect of zinc ions on caffeine-induced contracture in vascular smooth muscle and skeletal muscle of rat. *Cell Physiol Biochem* 12: 119–126, 2002.
14. **Choi KM, Zhong Y, Hoit BD, Grupp IL, Hahn H, Dilly KW, Guatimosim S, Lederer WJ, and Matlib MA.** Defective intracellular Ca^{2+}

signaling contributes to cardiomyopathy in Type 1 diabetic rats. *Am J Physiol Heart Circ Physiol* 283: H1398–H1408, 2002.

15. **Coppey LJ, Gellett JS, Davidson EP, Dunlap JA, Lund DD, and Yorek MA.** Effect of antioxidant treatment of streptozotocin-induced diabetic rats on endoneurial blood flow, motor nerve conduction velocity, and vascular reactivity of epineurial arterioles of the sciatic nerve. *Diabetes* 50: 1927–1937, 2001.

16. **Cousins RJ.** Absorption, transport, and hepatic metabolism of copper and zinc: special reference to metallothionein and ceruloplasmin. *Physiol Rev* 65: 238–309, 1985.

17. **Da Ros R, Assaloni R, and Ceriello A.** Antioxidant therapy in diabetic complications: what is new? *Curr Vasc Pharmacol* 2: 335–341, 2004.

18. **Dhalla NS, Liu X, Panagia V, and Takeda N.** Subcellular remodeling and heart dysfunction in chronic diabetes. *Cardiovasc Res* 40: 239–247, 1998.

19. **Dineley KE, Richards LL, Votyakova TV, and Reynolds IJ.** Zinc causes loss of membrane potential and elevates reactive oxygen species in rat brain mitochondria. *Mitochondrion* 5: 55–65, 2005.

20. **Ezaki O.** The insulin-like effects of selenate in rat adipocytes. *J Biol Chem* 265: 1124–1130, 1990.

21. **Fang ZY, Prins JB, and Marwick TH.** Diabetic cardiomyopathy: evidence, mechanisms, and therapeutic implications. *Endocr Rev* 25: 543–567, 2004.

22. **Foyer CH, Theodoulou FL, and Delrot S.** The functions of inter- and intra- cellular glutathione transport systems in plants. *Trends Plant Sci* 6: 486–492, 2001.

23. **Fructaci A, Kajstura J, Chimenti C, Jakoniuk I, Nadal-Ginard B, Maseri A, Nadal-Ginard B, and Anversa P.** Myocardial cell death in human diabetes. *Circ Res* 87: 1123–1132, 2000.

24. **Ghosh R, Mukherjee B, and Chatterjee M.** A novel effect of selenium on streptozotocin-induced diabetic mice. *Diabetes Res* 25: 165–171, 1994.

25. **Haase H and Maret W.** A differential assay for the reduced and oxidized states of metallothionein and thionein. *Anal Biochem* 333: 19–26, 2004.

26. **Haase H and Maret W.** Intracellular zinc fluctuations modulate protein tyrosine phosphate activity in insulin/insulin-like growth factor-1 signaling. *Exp Cell Res* 291: 289–298, 2003.

27. **Hayat SA, Patel B, Khattar RS, and Malik RA.** Diabetic cardiomyopathy: mechanisms, diagnosis and treatment. *Clin Sci (Lond)* 107: 539–557, 2004.

28. **Hei YJ, Farahbakhshian S, Chen X, Battell ML, and McNeill J.** Stimulation of MAP kinase and S6 kinase by vanadium and selenium in rat adipocytes. *Mol Cell Biochem* 178: 367–375, 1998.

29. **Hersfinkel M, Moran A, Grossman N, and Sekler I.** A zinc-sensing receptor triggers the release of intracellular Ca^{2+} and regulates ion transport. *Proc Natl Acad Sci USA* 98: 11749–11754, 2001.

30. **Ishikawa T, Kajiwara H, and Kurihara S.** Alterations in contractile properties and Ca^{2+} handling in streptozotocin-induced diabetic rat myocardium. *Am J Physiol Heart Circ Physiol* 277: H2185–H2194, 1999.

31. **Jacob C, Maret W, and Vallee BL.** Control of zinc transfer between thionein, metallothionein, and zinc proteins. *Proc Natl Acad Sci USA* 95: 3489–3494, 1998.

32. **Kajstura J, Fiordaliso F, Andreoli AM, Li B, Chimenti S, Medow MS, Limana F, Nadal-Ginard B, Nadal-Ginard B, and Anversa P.** IGF-1 overexpression inhibits the development of diabetic cardiomyopathy and angiotensin II-mediated oxidative stress. *Diabetes* 50: 1414–1424, 2001.

33. **Kang YJ.** The antioxidant function of metallothionein in the heart function. *Proc Soc Exp Biol Med* 222: 263–273, 1999.

34. **Keppler D.** Export pumps for glutathine S-conjugates. *Free Radic Biol Med* 27: 985–991, 1999.

35. **Kim D, Joe CO, and Han PL.** Extracellular and intracellular glutathione protects astrocytes from Zn^{2+}-induced cell death. *Neuroreport* 14: 187–190, 2003.

36. **Korichneva I, Hoyos B, Chua R, Levi E, and Hammmerling U.** Zinc release from protein kinase C as the common event during activation by lipid second messenger or reactive oxygen. *J Biol Chem* 277: 44327–44331, 2002.

37. **Li S, Li X, and Rozanski GJ.** Regulation of glutathione in cardiac myocytes. *J Mol Cell Cardiol* 35: 1145–1152, 2003.

38. **Liang Q, Carlson EC, Donthia RV, Kralik PM, Shen X, and Epstein PN.** Overexpression of metallothionein reduces diabetic cardiomyopathy. *Diabetes* 51: 174–181, 2002.

39. **Lowry OH, Rosebrough NJ, Farr AL, and Randall RJ.** Protein measurement with the folin phenol reagent. *J Biol Chem* 193: 265–275, 1951.

40. **Malaiyandi LM, Dineley KE, and Reynolds IJ.** Divergent consequences arise from metallothionein overexpression in astrocytes: zinc buffering and oxidant-induced zinc release. *Glia* 45: 346–353, 2004.

41. **Maret W.** Crosstalk of the group IIa and IIb metals calcium and zinc in cellular signaling. *Proc Natl Acad Sci USA* 98: 12325–12327, 2001.

42. **Maret W.** Metallothionein/disulfide interactions, oxidative stress, and the mobilization of cellular zinc. *Neurochem Int* 27: 111–117, 1995.

43. **Marfella R, Verrazzo G, Acampora R, La Marca C, Giunta R, Lucarelli C, Paolisso G, Ceriello A, and Giugliano D.** Glutathione reserves systemic hemodynamic changes by acute hyperglycemia in healthy subjects. *Am J Physiol Endocrinol Metab* 268: E1167–E1173, 1995.

44. **Mukherjee B, Anbszhagan S, Roy A, Ghosh R, and Chatterjee M.** Novel implications of the potential role of selenium on antioxidant status in streptozotocin-induced diabetic mice. *Biomed Pharmacother* 52: 89–95, 1998.

45. **Musat S, Wang X, and Dhalla NS.** Modification of the ATP-induced increase in $[Ca^{2+}]_i$ by copper and zinc in rat cardiomyocytes. *J Cardiovasc Pharmacol Ther* 3: 291–298, 1998.

46. **Nasu T.** Zinc ions block the intracellular calcium release induced by caffeine in guinea-pig taenia caeci. *Experientia* 51: 113–116, 1995.

47. **Nebot C, Moutet M, Huet P, Xu JZ, Yadan JC, and Chaudiere J.** Spectrophotometric assay of superoxide dismutase activity based on the activated autoxidation of a tetracyclic catechol. *Anal Biochem* 214: 442–451, 1993.

48. **Noda N, Hayashi H, Miyata H, Suzuki S, Kobayashi A, and Yamazaki N.** Cytosolic Ca^{2+} concentration and pH of diabetic rat myocytes during metabolic inhibition. *J Mol Cell Cardiol* 24: 435–446, 1992.

49. **Pacher P, Liaudet L, Soriano FG, Mabley JG, and Szabo E.** The role of poly(ADP-Ribose) polymerase activation in the development of myocardial and endothelial dysfunction in diabetes. *Diabetes* 51: 514–521, 2002.

50. **Pacher P, Obrosova IG, Mabley JG, and Szabo C.** Role of nitrosative stress and peroxynitrite in the pathogenesis of diabetic complications. Emerging new therapeutical strategies. *Curr Med Chem* 12: 267–275, 2005.

51. **Paglia DE and Valentine WN.** Studies on the quantitative and qualitative characterization of erythrocyte glutathione peroxidase. *J Lab Clin Med* 70:158–169, 1967.

52. **Schaffer G, Wascher TC, Kostner GM, and Graier WF.** Alterations in platelet Ca^{2+} signaling in diabetic patients are due to increased formation of superoxide anions and reduced nitric oxide production. *Diabetologia* 42: 167–176, 1999.

53. **Scheuhammer AM and Cherian MG.** Quantification of metallothioneins by a silver saturation method. *Toxicol Appl Pharmacol* 82: 417–425, 1986.

54. **Stapleton SR, Garlock G, Foellmi-Adam L, and Kletzien RF.** Selenium: potent stimulator of tyrosyl phosphorylation and activator of MAP kinase. *Biochim Biophys Acta* 1355: 259–269, 1997.

55. **Szabo C, Zanchi A, Komjati K, Pacher P, Krolewski AS, Quist WC, LoGerfo FW, Horton ES, and Veves A.** Poly(ADP-Ribose) polymerase is activated in subjects at risk of developing type 2 diabetes and is associated with impaired vascular reactivity. *Circulation* 106: 2680–2686, 2002.

56. **Tatsumi T and Fliss H.** Hypochlorous acid mobilizes intracellular zinc in isolated rat heart myocytes. *J Mol Cell Cardiol* 26: 471–479, 1994.

57. **Turan B, Fliss H, and Desilets M.** Oxidants increase intracellular free Zn^{2+} concentration in rabbit ventricular myocytes. *Am J Physiol Heart Circ Physiol* 272: H2095–H2106, 1997.

58. **Ulusu NN and Turan B.** Beneficial effects of selenium on some enzymes of diabetic rat heart. *Biol Trace Elem Res* 103: 207–215, 2005.

59. **Vega MT, Villalobos C, Garrido B, Gandia L, Bulbena O, Garcia-Sancho J, Garcia AG, and Artalejo AR.** Permeation by zinc of bovine chromaffin cell calcium channels: relevance to secretion. *Pflügers Arch* 429: 231–239, 1994.

60. **Viarengo A and Nicotera P.** Possible role of Ca^{2+} in heavy metal cytotoxicity. *Comp Biochem Physiol* 100C: 81–84, 1991.

61. **Wang H, Wei QQ, Cheng XY, Chen KY, and Zhu PH.** Inhibition of ryanodine binding to sarcoplasmic reticulum vesicles of cardiac muscle by Zn^{2+} ions. *Cell Physiol Biochem* 11: 83–92, 2001.

62. **Xu Z, Patel KP, Lou MF, and Rozanski GJ.** Up-regulation of K^+ channels in diabetic rat ventricular myocytes by insulin and glutathione. *Cardiovasc Res* 53: 80–88, 2002.

63. **Ye G, Metreveli NS, Ren J, and Epstein PN.** Metallothionein prevents diabetes-induced deficits in cardiomyocytes by inhibiting reactive oxygen species production. *Diabetes* 52: 777–783, 2003.

64. **Yu JZ, Rodrigues B, and McNeill JH.** Intracellular calcium levels are unchanged in the diabetic heart. *Cardiovasc Res* 34: 91–98, 1997.